



The dependence of percolation threshold on doping degree in $\text{La}_{1-x}(\text{K}, \text{Ag})_x\text{MnO}_3$ manganites

A.G. Gamzatov*, I.K. Kamilov

Amirkhanov Institute of Physics, Daghestan Scientific Center of RAS, 367003 Makhachkala, Russia

ARTICLE INFO

Article history:

Received 26 August 2011

Received in revised form 13 October 2011

Accepted 14 October 2011

Available online 24 October 2011

PACS:

75.47.Lx

75.47.Gk

Keywords:

Manganite

Colossal magnetoresistance

Percolation

ABSTRACT

Experimental results and the analysis of a resistivity of $\text{La}_{1-x}(\text{K}, \text{Ag})_x\text{MnO}_3$ manganites are presented. The behavior of the resistivity $\rho(T)$ in a wide temperature range and a phase transition region are described. For the description of $\rho(T)$ near a phase transition temperature are used the representations of the percolation theory. A percolation threshold dependence on doping degree in $\text{La}_{1-x}(\text{K}, \text{Ag})_x\text{MnO}_3$ manganites is studied. In $\text{La}_{1-x}\text{K}_x\text{MnO}_3$ system for samples with $x \leq 0.12$, an infinite conductivity channel forms at temperatures below the Curie temperature, and with $x > 0.12$ of potassium concentrations it is appeared at $T > T_C$.

© 2011 Elsevier B.V. All rights reserved.

1. Introduction

Manganites doped by univalent ions (Na, K, Ag) have a number of essential distinctions as compared with well-explored manganites $\text{Ln}_{1-x}\text{A}_x\text{MnO}_3$, where A is a divalent metal (Ca, Sr, ...). When doping a maternal composition LaMnO_3 by univalent ions of Ag^+ , K^+ , in order to keep the charge balance, it is needed that two ions of Mn^{3+} change into Mn^{4+} per every introduced univalent ion of Ag^+ , K^+ , what means the narrowing of phase diagram $T-x$ along the x axis and high values for T_C at low doping degree ($x < 0.2$). The merit of these manganites is a high sensitivity of their physical properties to the magnetic field, large colossal magnetoresistance effect (CMR) [1–9] and magnetocaloric effect (MCE) observed in the vicinity of room temperatures [10–14]. Moreover, the manganites belong to systems with strongly correlated electron properties, where a strong interconnection reveals between the electron, magnetic, and lattice subsystems of a solid state. This implies that there is a direct functional connection between the parameters describing these subsystems [15,16].

Even so, univalent manganites still remain less studied materials than manganites doped by divalent metal. The reasons for this, first

of all, are technological difficulties in a production of high-quality ceramic samples because of the thermal instability; to receive the monocrystalline samples seems to be impossible at all.

Available literature information on the experimental results of electrical properties of $\text{La}_{1-x}\text{Ag}_x\text{MnO}_3$ [1–6,17] and $\text{La}_{1-x}\text{K}_x\text{MnO}_3$ [7–9] manganites is rather contradictory. First of all this is connected with that the manganites doped by univalent ions can be synthesized only by ceramic technology, what implicates a strong dependency of the properties on technological parameters ($P(\text{O}_2)$, T , t).

Earlier we have carefully studied the structural and magnetocaloric properties of $\text{La}_{1-x}\text{Ag}_x\text{MnO}_3$ [12] and $\text{La}_{1-x}\text{K}_x\text{MnO}_3$ [14] manganites. We attend sufficient attention to electrical properties of $\text{La}_{1-x}\text{Ag}_x\text{MnO}_3$ system that described in [4,16,18–20]. The works [16,19,20] are devoted to the quantitative analysis of the resistivity in $\text{La}_{1-x}\text{Ag}_x\text{MnO}_3$ species within temperature intervals 4–350 K. The $\rho(T)$ behavior close to the metal–insulator transition temperature is described within the framework of the percolation theory well enough. In this manuscript, the temperature dependence of the resistivity for $\text{La}_{1-x}\text{K}_x\text{MnO}_3$ ($x = 0.05; 0.1; 0.11; 0.13; 0.15$ and 0.175) system is analyzed similarly; a comparative analysis with the results derived earlier for $\text{La}_{1-x}\text{Ag}_x\text{MnO}_3$ species are presented. As opposed to our previous works, in this one, we endeavour to explain an origination of additional peaks in curve and to analyze the temperature dependence of ferromagnetic phase volume fraction.

* Corresponding author.

E-mail address: gamzatov_adler@mail.ru (A.G. Gamzatov).

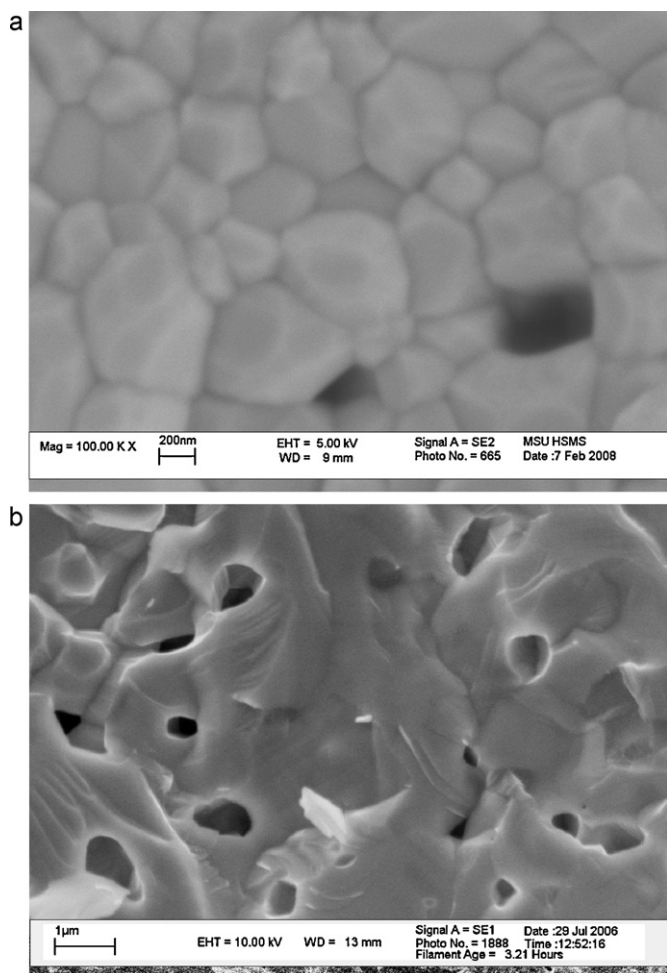


Fig. 1. Scanning electron microscopy data. The picture of surface: (a) for $\text{La}_{0.87}\text{K}_{0.13}\text{MnO}_3$, and (b) $\text{La}_{0.85}\text{Ag}_{0.15}\text{MnO}_3$.

2. Results and discussion

$\text{La}_{1-x}(\text{K}, \text{Ag})_x\text{MnO}_3$ compounds are ceramic samples. A synthesis processing and characteristics were described in work [4] for $\text{La}_{1-x}\text{Ag}_x\text{MnO}_3$ and in [14] for $\text{La}_{1-x}\text{K}_x\text{MnO}_3$. The main parameters of annealing for samples of $\text{La}_{1-x}\text{Ag}_x\text{MnO}_3$ were $T = 1100^\circ\text{C}$, $P(\text{O}_2) = 1 \text{ atm}$, $t = 25 \text{ h}$; $\text{La}_{1-x}\text{K}_x\text{MnO}_3$ were synthesized at $T = 1000^\circ\text{C}$, $P(\text{O}_2) = 1 \text{ atm}$, $t = 30 \text{ h}$. X-ray analysis data indicated that the received samples were univalent rhombohedral distorted perovskites and belonged to the spatial group $R\bar{3}c$. The ceramics had a homogeneous grained structure with a pellet mean size of 100–300 nm for $\text{La}_{1-x}\text{K}_x\text{MnO}_3$ and 1 μm for $\text{La}_{1-x}\text{Ag}_x\text{MnO}_3$ (Fig. 1a and b).

The samples, produced by a ceramic technology, possess the submicron sizes of pellets, and transport properties of such ceramics are defined by the pellet boundaries. An expression for the resistance of such samples is $\rho = \rho_0 + (L_1/L_0)\rho_1$, where ρ_0 means a crystallite resistance with mean size L_0 , ρ_1 is a pellet boundary resistance with mean width L_1 . As a rule $\rho_1 \gg \rho_0$. As was shown in [21] the resistance of ceramic samples of La–Sr–Mn–O increases more than in 5 orders of magnitude at decreasing of pellet sizes from 10 μm to 20 nm. This implies that a main contribution into the resistance magnitude make grain boundaries. In these samples, a metal–insulator phase transition is illegible spread maximum; a temperature of the maximum is considerably lower than T_C . The researches of inherent, undisguised by grain boundaries of

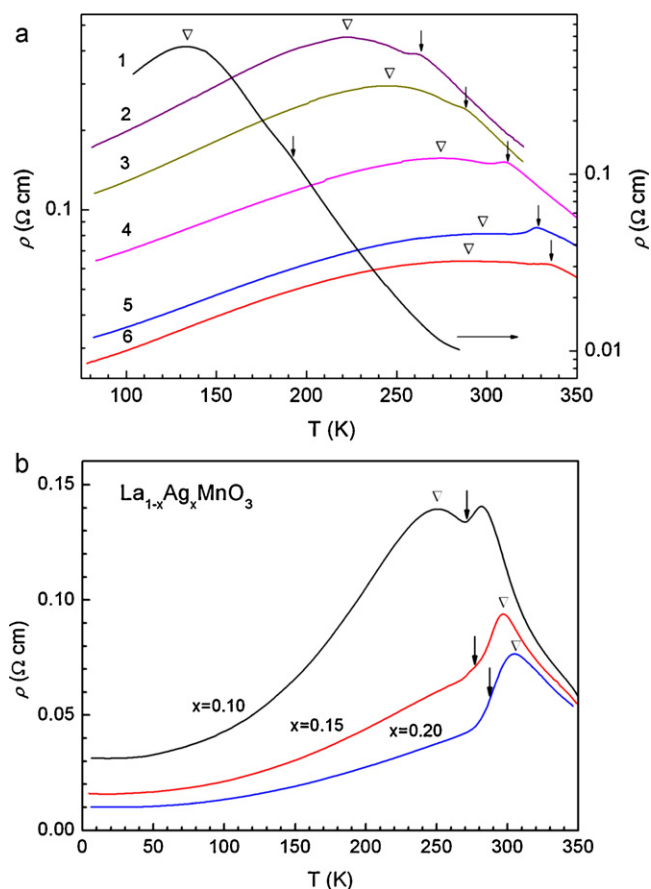


Fig. 2. Resistivity temperature dependence: (a) for $\text{La}_{1-x}\text{K}_x\text{MnO}_3$. Numbers of curves correspond to numbers of samples: 1 – $x = 0.05$; 2 – $x = 0.10$; 3 – $x = 0.11$; 4 – $x = 0.13$; 5 – $x = 0.15$ and 6 – $x = 0.175$. (b) For $\text{La}_{1-x}\text{Ag}_x\text{MnO}_3$. Arrows indicate the T_C , and ∇ denotes T_{max} .

manganites properties are required samples with sufficiently large (microns) pellet sizes and dense intergranular contacts.

Fig. 2 (a and b) demonstrates the experimental results on temperature dependences of the resistivity for $\text{La}_{1-x}\text{K}_x\text{MnO}_3$ ($x = 0.05$; 0.10; 0.11; 0.13; 0.15 and 0.175) and $\text{La}_{1-x}\text{Ag}_x\text{MnO}_3$ ($x = 0.10$; 0.15 and 0.20). As is evident from figures, a $\rho(T)$ behavior is of bell-shaped form, typical for other manganites: a metallic behavior is lower of some T_{max} , and semiconductive course is higher of T_{max} (T_{max} means a temperature under which $d\rho/dT$ changes the sign). However, there is an essential discrepancy that in $\text{La}_{1-x}\text{K}_x\text{MnO}_3$, except extended maximum at T_{max} , small humps are revealed at $T > T_{max}$. Double peaks are detected for some samples in $\text{La}_{1-x}\text{Ag}_x\text{MnO}_3$ system. Occurrence of two maxima in $\rho(T)$ curves of polycrystalline manganites is not rarity [1,4,6,22]. The simplest reason for that is a presence of structure and phase heterogeneities that can be eliminated by means of homogenizing [4,6]. But such explanation does not fit to the system of $\text{La}_{1-x}\text{K}_x\text{MnO}_3$, as the X-ray – structural and X-ray – phase analyses confirm the homogeneity of studied samples [14].

The in-depth physical processes underlying the occurrence of two maxima are not detected finally; in any event, it was lively discussed in literature [1,23,24]. Authors [1] explained the $\rho(T)$ dependence for $\text{La}_{1-x}\text{Ag}_x\text{MnO}_3$ ceramics using the model of a heterogeneous electron phase layering and argued in favor of that choice. E. Rozenberg [23], in his comments to the work [1], indicates that the interpretation of authors [1] is inconsistent, and such a behavior is explained by a grain boundaries effect.

The meaning of the effect consists in the following. Granular (polycrystalline) manganites are the heterogeneous systems: each

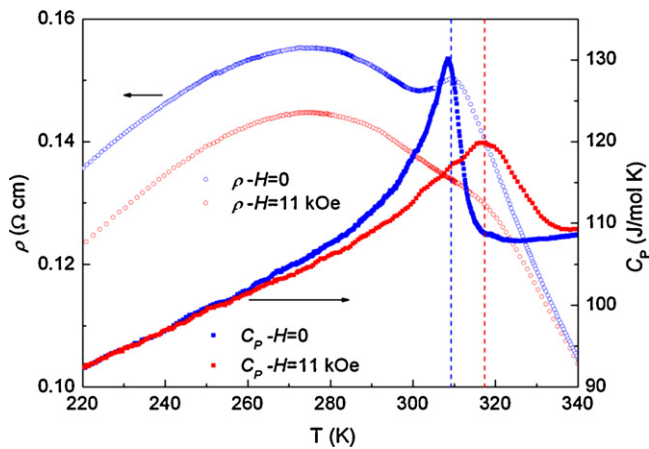


Fig. 3. The temperature dependence of the resistivity and heat capacity for $\text{La}_{0.87}\text{K}_{0.13}\text{MnO}_3$ at $H=0$ and $H=11$ kOe.

pellet should be considered as a grain consisting of a center with a certain T_C and the same near surface layer depleted by the charge carriers [25]. This layer is magnetically and structurally heterogeneous; it has its own very fuzzy critical temperature considerably lower than T_C . Under this reason, when falling the temperature, at first we observe a magnetic phase transition inside the pellets with T_C (humps on $\rho(T)$ dependence), and the intergranular layer continues to be in paramagnetic insulating state and is a barrier for charge carriers. When further decreasing the temperature, a magnetic ordering is formed in the intergranular space, which is attended by appearing of infinite conducting channel and a change in derivative of $d\rho/dT$.

The analysis of our experimental data show that they are on the scheme (Fig. 2). The humps on $\rho(T)$ curves observed at temperature falling agree precisely with T_C , which we defined as temperatures of magnetocaloric effect maximum at low values of a magnetic field [14], and with temperatures of CMR effect maximum, which usually coincide with T_C . A continued decrease in temperature induces a further increase in the resistivity, especially clear in weakly doped samples, notwithstanding the magnetic phase transition inside of pellets is finished already. Only at T_{max} , when the infinite conducting channel is formed in the system, the resistivity begins to fall. Furthermore, the behavior of additional peaks in the magnetic field is identical with the behavior of ferromagnetic heat capacity in the magnetic field, i.e. the field of 11 kOe mutes the anomaly and shifts a maximum temperature towards high temperatures by $\Delta T=8$ K both along $C_p(T, H)$ [26] and by $\rho(T, H)$ data (Fig. 3). All above mentioned and a regularity of their occurrence with K -concentration indicates that these additional maximums in $\rho(T)$ dependence are the appearance of the magnetic phase transition in $\text{La}_{1-x}\text{K}_x\text{MnO}_3$.

Fig. 2(b) presents the temperature dependence of the resistivity for $\text{La}_{1-x}\text{Ag}_x\text{MnO}_3$, which we studied in detail earlier [4,18–20]. Works [1,4,6] reported about a nature of additional maximums in $\text{La}_{1-x}\text{Ag}_x\text{MnO}_3$. Researches on transport properties of $\text{La}_{1-x}\text{Ag}_x\text{MnO}_3$ manganites [4,6,22] indicated that in some cases the same composition demonstrated two peaks on $\rho(T)$ dependence versus synthesis conditions ($P(\text{O}_2)$, T , t); in others it revealed only one, that also confirmed a technological nature of additional peaks occurrence.

As it is evident from Fig. 2 (a and b), $T_{MI} < T_C$ for $\text{La}_{1-x}\text{K}_x\text{MnO}_3$ species and $T_{MI} > T_C$ for $\text{La}_{1-x}\text{Ag}_x\text{MnO}_3$, an origination of such a behavior is not clear, most likely the reasons are in synthesis technology [4]. In the majority of monocrystalline manganites showing the metal–insulator transition, the temperatures, under which the magnetic ordering and metal conductivity appear, approximately agree with each other [27,28], what corresponds to a double

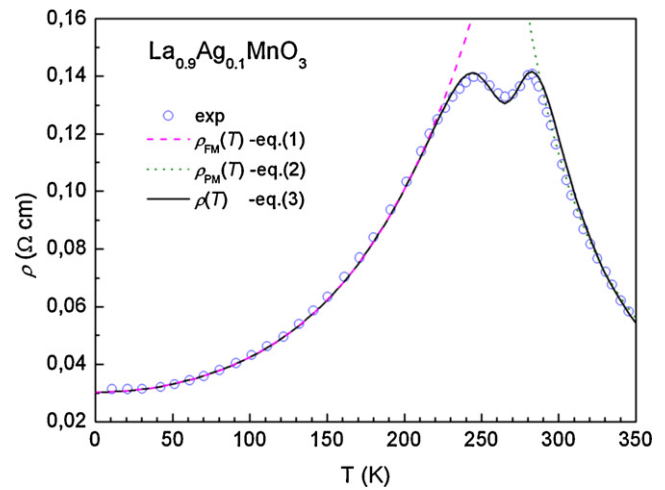


Fig. 4. Temperature dependence of $\text{La}_{0.9}\text{Ag}_{0.1}\text{MnO}_3$ resistivity. Dot line means the approximation by Eq. (1), dash and dot line is approximation by Eq. (2), solid line corresponds to data by Eq. (3).

exchange model, and any additional anomalies in $\rho(T)$ behavior are not found. However, it turned out that the same behavior is typical for monocrystalline manganites [29], but the $|T_{MI} - T_C|$ difference is substantially narrower than for ceramic samples. An existence of magnetic-biphase ferromagnetic and antiferromagnetic state excited by a strong s – d exchange can serve as one of possible reasons for such difference between T_C and T_{MI} in manganites [29,30].

For the sake of determination of the percolation threshold dependence on a concentration of doping elements we carried out a quantitative analysis for the resistivity temperature dependence of explored samples. In low-temperature ferromagnetic phase, the $\rho(T)$ dependence is approximated by an expression that includes several scattering mechanisms (dot line in Fig. 4):

$$\rho_{FM}(T) = \rho_0 + AT^2 + BT^{4.5} \quad (1)$$

where ρ_0 is the residual resistance, a term AT^2 is usually assigned to the mutual scattering of charge carriers, a term $BT^{4.5}$ is caused by electron–magnon processes of scattering. The $\rho(T)$ dependence above metal–insulator transition temperature is well approximated by the thermoactivation law (dash and dot line in Fig. 4):

$$\rho = DT \exp\left(\frac{E_p}{k_B T}\right) \quad (2)$$

where E_p implies the activation energy, D is a coefficient independent from T . Polarons of small radius serve as charge carriers in this region that implement the conductivity by jumping into the nearest free states. A detail description for values and meaning of approximation coefficients (ρ_0 , A , B , D , E_p) in Eqs. (1) and (2) and consequent conclusions were given in works [4,28].

Taking into account that metal–insulator transition has a percolation character and assuming that a competition between ferromagnetic and paramagnetic regions is of great importance in formation of the CMR effect a complete expression for the resistivity can be written in following way [31]:

$$\rho(T) = \rho_{FM}f + \rho_{PM}(1-f)$$

where f is the volume concentration of ferromagnetic (FM) phase, $(1-f)$ is the volume concentration of paramagnetic (PM) phase. The volume concentrations of FM and PM phases satisfy the Boltzman distribution:

$$f = \frac{1}{1 + \exp(\Delta U/k_B T)}$$

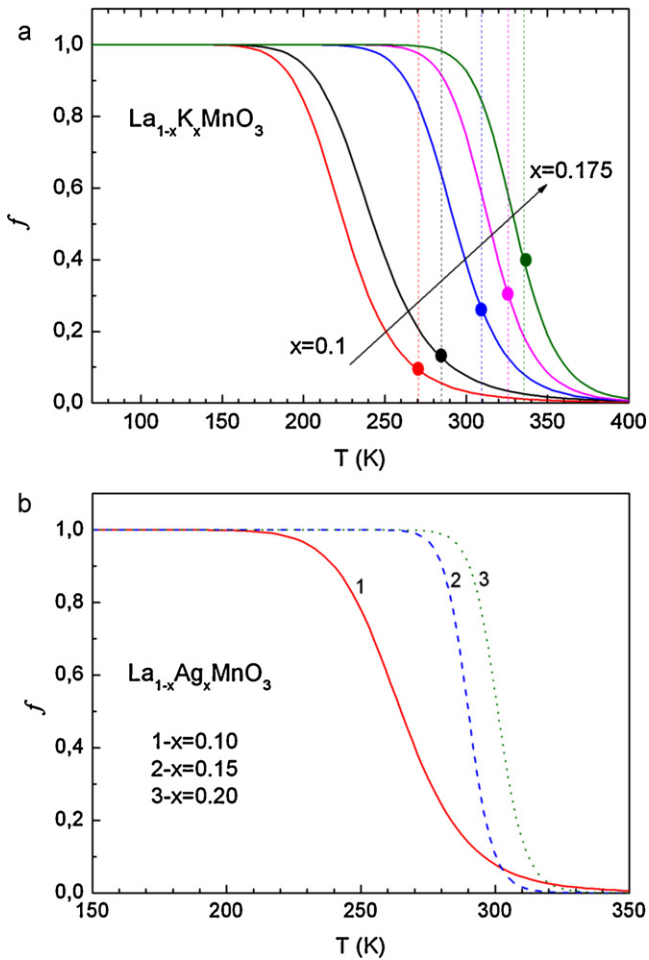


Fig. 5. The temperature dependence of ferromagnetic phase volume fraction for different samples: (a) for $\text{La}_{1-x}\text{K}_x\text{MnO}_3$ and (b) $\text{La}_{1-x}\text{Ag}_x\text{MnO}_3$. The points on $f(T)$ lines are the Curie temperature for corresponding samples.

where $\Delta U \sim -U_0(1 - T/T_{C1})$ implies an energy difference between FM and PM states, T_{C1} means a temperature in the vicinity of what the resistivity has a maximum value [31]. Then a complete expression describing the resistivity dependence as the temperature function is of the form:

$$\rho(T) = (\rho_0 + AT^2 + BT^{4.5})f + DT \exp\left(\frac{E_P}{k_B T}\right)(1 - f) \quad (3)$$

Results approximated by Eqs. (1)–(3) are presented in Fig. 4 for $\text{La}_{0.9}\text{Ag}_{0.1}\text{MnO}_3$. The same analysis of $\rho(T)$ dependence for $\text{La}_{1-x}\text{K}_x\text{MnO}_3$ and $\text{La}_{1-x}\text{Ag}_x\text{MnO}_3$ was shown in works [8,16,19]. As it is clear, the Eq. (3) describes the $\rho(T)$ behavior in a wide temperature range quite enough. Such an approximation does not imply a profound physics, but merely it is a form of mathematical description for $\rho(T)$ dependence, at the same time such calculations more clearly demonstrate the general laws what is shown below.

The temperature dependence of a ferromagnetic phase volume fraction $f(T)$, that is corresponds to reduced magnetization $f(T) = M/M_S$ at first approximation, can be estimated from the approximation of $\rho(T)$ data using Eq. (3) [16,19,32]. The $f(T)$ temperature dependence for all $\text{La}_{1-x}(\text{Ag}, \text{K})_x\text{MnO}_3$ samples is demonstrated in Fig. 5(a and b).

As follows from Fig. 2(a) the T_C exceeds T_{max} , i.e. $T_C > T_{max}$ for all $\text{La}_{1-x}\text{K}_x\text{MnO}_3$ samples. A qualitative explanation of observed systematic excess of T_C over T_{max} consists in following. The occurrence of ferromagnetic ordering at T_C roughly coincides with achieving of ferromagnetic phase critical volume (f), called the percolation

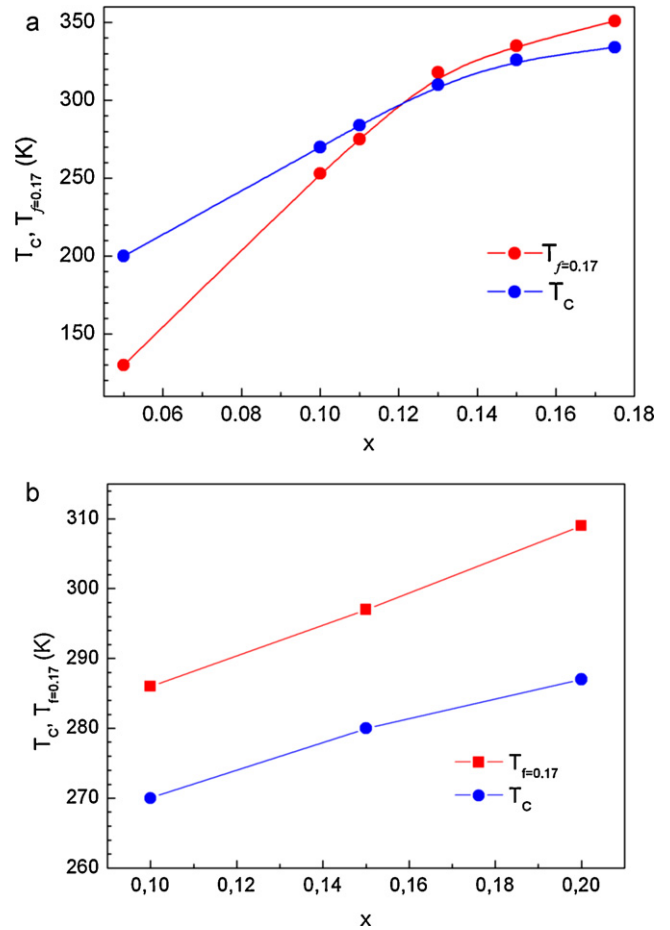


Fig. 6. The dependence of T_C and $T_f=0.17$ on concentration: (a) for $\text{La}_{1-x}\text{K}_x\text{MnO}_3$ and (b) for $\text{La}_{1-x}\text{Ag}_x\text{MnO}_3$.

threshold, in which an infinite percolation channel ($f=0.16-0.31$) is formed [33,34]. The rest of the sample volume ($1 - f$) still remains in an insulator state, for which the $\rho(T)$ dependence has a semi-conducting character ($d\rho/dT < 0$). The derivative changes a sign and the metallic conductivity starts, i.e. the metal-insulator transition occurs only after achieving $f \geq 0.5$, when the ferromagnetic phase volume exceeds the insulator phase. A competition between these two mechanisms of conductivity brings us to the observed dependence of $\rho(T)$. In this connection we mention a work [22] where the authors detected the T_C dependence on the pellet sizes for $\text{La}_{0.9}\text{Te}_{0.1}\text{MnO}_3$. They show that T_C and T_{MI} approximately coincided with each other for the samples with pellet mean sizes of 53, 82 and 120 nm; when further decreasing in pellet sizes (~ 40 nm) $T_C = 268$ K, $T_{MI} = 222$ K. Such sharp rise of T_C with pellet sizes loss, the authors attributed to the growth of valence angle of Mn–O–Mn. In principle, such a mechanism could be underlain the difference between T_C and T_{MI} for La–(K, Ag)–Mn–O, however it is unlikely, as a mean size of pellets was 100–300 nm for $\text{La}_{1-x}\text{K}_x\text{MnO}_3$ system and 1 μm for $\text{La}_{1-x}\text{Ag}_x\text{MnO}_3$ system.

In Fig. 5(a and b), a shaded area involves an interval, in which an infinite percolation channel can be occurred in manganites. The thick dots on $f(T)$ diagrams imply the Curie temperature for all corresponding samples. As follows from Fig. 5(a), the infinite channel is formed at temperature below the Curie temperature for $\text{La}_{1-x}\text{K}_x\text{MnO}_3$ system with $x \leq 0.12$ and when K-concentration is $x > 0.12$ at $T > T_C$.

Graphically it is presented in Fig. 6(a), where the dependence of the Curie temperature (T_C) and $T_f=0.17$ on potassium concentration for the $\text{La}_{1-x}\text{K}_x\text{MnO}_3$ is shown, ($T_f=0.17$ is a temperature

under which the infinite conductive cluster forms). Fig. 6(b) displays the dependence of T_C and $T_f = 0.17$ on silver concentration for $\text{La}_{1-x}\text{Ag}_x\text{MnO}_3$, whence shows that $T_C > T_f = 0.17$ for all samples. A distinction in the dependence of $T_f = 0.17$ on concentration of doping elements in $\text{La}_{1-x}\text{K}_x\text{MnO}_3$ and $\text{La}_{1-x}\text{Ag}_x\text{MnO}_3$ is a consequence of different sizes of the pellets most likely.

So, the temperature and concentration dependences of the resistivity are studied for $\text{La}_{1-x}\text{K}_x\text{MnO}_3$ and $\text{La}_{1-x}\text{Ag}_x\text{MnO}_3$ samples. The anomalies, connected with paramagnetic–ferromagnetic transition, are detected on $\rho(T)$ dependence in $\text{La}_{1-x}\text{K}_x\text{MnO}_3$ over metal–insulator transition temperature, and $T_{max} < T_C$ for all samples. The mechanisms of carriers scattering in ferromagnetic, paramagnetic phases and the dependence of ferromagnetic phase volume on a change in temperature are determined.

Acknowledgements

Author appreciates A. Batdalov's, A. Aliev's and E. Rosenberg's attention to the work and useful remarks and also A.C. Mankevich for kindly provided samples. This work was partly supported by RFBF (Grant Number 09-08-96533, 11-02-01124) and the Physics Department of RAS.

References

- [1] S.L. Ye, W.H. Song, J.M. Dai, K.Y. Wang, S.G. Wang, C.L. Zhang, J.J. Du, Y.P. Sun, J. Fang, *Journal of Magnetism and Magnetic Materials* 248 (2002) 26.
- [2] S. Ravi, M. Kar, *Physica B* 348 (2004) 169.
- [3] M. Battabyal, T.K. Dey, *Physica B* 367 (2005) 40.
- [4] I.K. Kamilov, A.G. Gamzatov, A.M. Aliev, A.B. Batdalov, Sh.B. Abdulvagidov, O.V. Melnikov, O.Y. Gorbenko, A.R. Kaul, *Journal of Experimental and Theoretical Physics* 105 (2007) 774.
- [5] M. Kar, S. Ravi, *Material Science Engineering B* 110 (2004) 46.
- [6] L. Pi, M. Hervieu, A. Maignan, C. Martin, B. Raveau, *Solid State Communications* 126 (2003) 229.
- [7] S. Das, T.K. Dey, *Journal of Magnetism and Magnetic Materials* 294 (2005) 338.
- [8] S. Das, T.K. Dey, *Solid State Communications* 134 (2005) 837.
- [9] S. Das, T.K. Dey, *Physica B* 381 (2006) 280–288.
- [10] T. Tang, K.M. Gu, Q.Q. Cao, D.H. Wang, S.Y. Zhang, Y.W. Du, *Journal of Magnetism and Magnetic Materials* 222 (2000) 110.
- [11] N.T. Hien, N.P. Thuy, *Physica B* 319 (2002) 168.
- [12] I.K. Kamilov, A.G. Gamzatov, A.M. Aliev, A.B. Batdalov, A.A. Aliverdiev, Sh.B. Abdulvagidov, O.V. Melnikov, O.Y. Gorbenko, A.R. Kaul, *Journal of Physics D: Applied Physics* 40 (2007) 4413.
- [13] S. Das, T.K. Dey, *Journal of Alloys and Compounds* 440 (2006) 30.
- [14] A.M. Aliev, A.G. Gamzatov, A.B. Batdalov, A.S. Mankevich, I.E. Korsakov, *Physica B* 406 (2011) 885.
- [15] A.G. Gamzatov, A.B. Batdalov, *Physica B* 406 (2011) 1902.
- [16] A.G. Gamzatov, A.B. Batdalov, A.R. Kaul, O.V. Melnikov, *Physics of the Solid State* 53 (2011) 182.
- [17] V.P.S. Awana, R. Tripathi, S. Balamurugan, H. Kishan, E. Takayama-Muromachi, *Solid State Communications* 140 (2006) 410.
- [18] I.K. Kamilov, A.G. Gamzatov, A.M. Aliev, A.B. Batdalov, Sh.B. Abdulvagidov, O.V. Melnikov, O.Y. Gorbenko, A.R. Kaul, *Low Temperature Physics* 33 (2007) 829.
- [19] A.G. Gamzatov, A.B. Batdalov, *Phase Transitions* 83 (2010) 343.
- [20] A.G. Gamzatov, A.B. Batdalov, I.K. Kamilov, *Physica B* 406 (2011) 2231.
- [21] L. Balcells, J. Foncuberta, B. Martínez, X. Obradors, *Physical Review B* 58 (1998) R14697.
- [22] J. Yang, B.C. Zhao, R.L. Zhang, Y.Q. Ma, Z.G. Sheng, W.H. Song, Y.P. Sun, *Solid State Communications* 132 (2004) 83.
- [23] E. Rozenberg, *Journal of Magnetism and Magnetic Materials* 270 (2004) 237.
- [24] S.L. Ye, W.H. Song, J.M. Dai, K.Y. Wang, S.G. Wang, C.L. Zhang, J.J. Du, Y.P. Sun, J. Fang, *Journal of Magnetism and Magnetic Materials* 270 (2004) 244–246.
- [25] B.I. Belevtsev, D.G. Naugle, K.D.D. Rathnayaka, A. Parasiris, J. Fink-Finowicki, *Physica B* 355 (2005) 341.
- [26] A.M. Aliev, A.G. Gamzatov, A.B. Batdalov, A.S. Mankevich, I.E. Korsakov, *Journal of Experimental and Theoretical Physics* 112 (2011) 461.
- [27] N.G. Bebenin, *Physics of Metals and Metallography* 111 (2011) 236.
- [28] A. Urushibara, Y. Moritomo, T. Arima, A. Asamitsu, G. Kido, Y. Tokura, *Physical Review B* 51 (1995) 14103–14109.
- [29] R.V. Pomortsev, A.V. Korolev, V.E. Arkhipov, V.P. Dyakina, *JETP Letters* 74 (2001) 28.
- [30] R.V. Demin, O. Yu Gorbenko, A.R. Kaul, L.I. Koroleva, O.V. Melnikov, A.Z. Muminov, R. Szymczak, M. Baran, *Physics of the Solid State* 47 (2005) 2287.
- [31] G. Li, H.-D. Zhou, S.J. Feng, *Journal of Applied Physics* 92 (2002) 1406–1410.
- [32] M. Jaime, P. Lin, S.H. Chun, M.B. Salamon, P. Dorsey, M. Rubinstein, *Physical Review B* 60 (1999) 1028.
- [33] L.P. Gor'kov, *Physics Uspekhi* 41 (1998) 589.
- [34] A.B. Khanikaev, A.B. Granovskii, J.P. Clerc, *Physics of the Solid State* 44 (2002) 1611.